

Reducing motion noise in marine magnetotelluric measurements by means of tilt records

Anne Neska,¹ Krzysztof Nowożyński,¹ Jan Reda¹ and Marion Jegen-Kulcsar²

¹*Institute of Geophysics PAS, ul. Ks. Janusza 64, 01-452 Warszawa, Poland. E-mail: anne@igf.edu.pl*

²*GEMAR – Helmholtz Centre for Ocean Research Kiel, East Shore Campus, Wischhofstr. 1-3, D-24148 Kiel, Germany*

Accepted 2013 March 4. Received 2013 March 1; in original form 2012 October 24

SUMMARY

The analysis of marine magnetotelluric data is often complicated by disturbing signals that are caused by small-scale periodic movements of the instrument. The motion-induced noise leads to a bias and/or severe scattering in the derived magnetotelluric transfer functions. Both the motion itself and its effects on the magnetic and telluric time-series are investigated in this study using an 80 d magnetotelluric data set that includes dynamic tilt records measured in the Pacific Ocean off Costa Rica. We apply a standard motion removal technique as well as a newly developed method to correct for motion-induced noise. The resulting magnetotelluric transfer functions are of significantly better quality than the uncorrected ones. Furthermore, the study of the properties of motion noise leads to conclusions about the optimal processing approach even in case of data sets where an explicit correction for that noise is not possible.

Key words: Time-series analysis; Magnetotellurics; Pacific Ocean.

1 INTRODUCTION

Marine magnetotelluric measurements require the recording of electric and magnetic field variations, related to induction processes in the Earth, on the seafloor. For this purpose a buoyant instrument frame is equipped with the magnetic and electric field sensors, a synchronized high precision clock and a data logger. The frame is made negatively buoyant through an anchor weight, which is attached below the frame by a release mechanism, and the instrument is deployed free falling from the ship. After the measurement, the anchor is released through an acoustic signal and the instrument rises to the surface and is recovered.

The strength of magnetic field variations on the seafloor related to the desired induction effects ranges from about one nT to hundreds of nT depending on frequency and strength of the ambient source field, which is related to space weather conditions. Magnetotelluric fields at the seafloor usually have a much smaller signal strength than concurrent fields on land due to the absorption of electromagnetic energy by the overlying ocean. Small movements of the magnetic sensor by less than a hundredth of a degree through the strong magnetic dipole field of the Earth will cause a signal (motion induced signal) that is unrelated to the induction process in the Earth, but of the same order of magnitude as the relevant signals.

A precise measurement of electric and magnetic fields requires a stable instrument platform on the seafloor. However, the required stability might not always be reached for a variety and combination of reasons. The deployment procedure precludes a control of the exact landing position (usually within a region of a tenth of the

water depth depending on instrument design and prevailing ocean currents), which is a problem especially in rougher terrains without much sediment cover. Secondly, the instrument is subjected to motion-induced noise through ocean and tidal currents and waves, which depending on water depth and location may be very large. Most marine MT instrumentations are equipped with a coarse tilt meter used to measure the static tilt of the instrument on the seafloor. Nowadays many groups also employ high-resolution tiltmeters and they sample tilt variations synchronously with magnetotelluric fields. However, the relationship between tilt and both magnetic and electric field variations is actually quite complex, as will be shown in this paper, which explains why no simple removal techniques for motion-induced noise exist to date. The only work on this topic known to us has been presented by Lezaeta *et al.* (2005). Most observations reported there are similar to ours, whereas we differ in some conclusions on the generation of motion noise. The removal technique proposed by the authors which proved successful for data affected by moderate motion noise failed when applied to the data set considered here (Worzewski 2011).

The effect of motion induced noise in marine magnetotelluric data presented here is based on a magnetotelluric (and tilt) data set acquired offshore the coast of Costa Rica. The data set has been collected in the framework of the collaborative research project SFB574 ‘Volatiles and Fluids in Subduction Zones’ in 2007 to image the hydration and dehydration cycle of a subduction zone (Worzewski *et al.* 2011). Data acquisition and interpretation was particularly challenging as (a) the measurement occurred during a minimum in the solar cycle which is associated with very weak source fields, (b) the data were recorded prevalently at large water

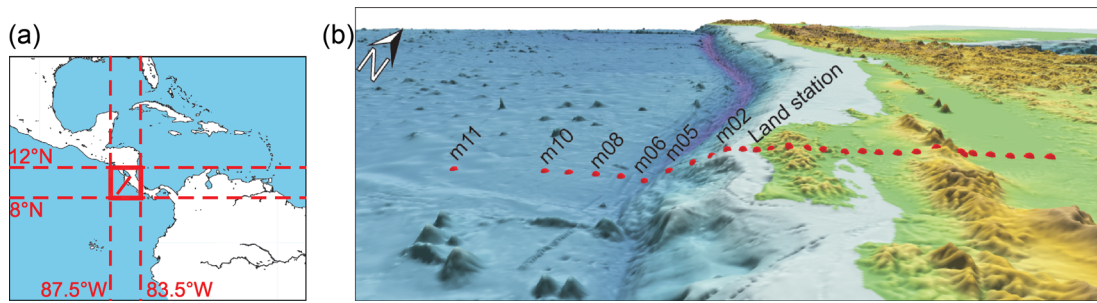


Figure 1. Overview map: (a) study area in the Pacific Ocean and Costa Rica with profile, (b) sketch of site locations and site depths on profile. Offshore sites m03, m04 and m05 and the westernmost onshore site as reference are included in this work. Figure after Worzewski (2011), modified.

depth (maximum depth: 3.8 km), such that the signal strength was further reduced through the skin effect of the overlying ocean, (c) imaging of the subduction zone required a profile crossing the continental shelf characterized by strong topography and strong tidal currents that break on the shelf and (d) first generation type of instrumentation was used in the data acquisition. Although the first generation instrumentation was already equipped with a tiltmeter that was sampling synchronously with the electromagnetic field data, first attempts to reduce motion-induced noise by means of tiltmeter data failed (Worzewski 2011). However, the tiltmeter data allowed for an unambiguous identification of the tilt motion which were used for further processing. Sufficiently precise magnetotelluric transfer functions could be derived from the data sets due to the length of the time-series (80 d) and a land reference station.

The aim of this study is to use these data and to present an analysis of the tilt motion and its effects on magnetic and telluric data (Section 2), to show that motion noise on magnetic channels can be dramatically reduced by means of known and new correction methods (Section 3), and to demonstrate that finally, good-quality sounding curves can be obtained from motion-noise affected marine MT data even without the time-consuming and somewhat subjective work of manual data selection applied in Worzewski (2011; Section 4).

2 TILT MOTION AND ITS EFFECTS ON MAGNETOTELLURIC DATA

2.1 Tilt motion

The strength of the tilt motion depends on a series of factors that will be outlined in the following. Some introductory remarks on the profile structure will be necessary to illustrate this complex pattern: The profile runs perpendicular to the Pacific coast and consists of one onshore reference and 11 marine stations that are numbered consecutively. Site m01 is situated closest to the coast at the shallowest water depth. The profile continues descending the continental slope, crosses the trench and ends at station m11 *ca.* 180 km off the coast in the deep ocean (Fig. 1).

2.1.1 Water depth/bathymetry

A common feature of the tilt records of all stations is a more or less constant offset amounting to not more than a few degrees. It reflects the not completely horizontal position of the instrument on the seafloor. This is expected in the context of marine magnetotellurics. A transformation of the magnetic data into a horizontal coordinate system is necessary then, it is done by appropriate rotations (*cf.* Fitterman & Yin 2004; Nowożyński 2005) basing on both static tilt

angles. As long as these static offsets are the only main feature of the tilt records, there does not exist a motion noise problem, and data can be subjected to further processing like onshore ones after the levelling operations and maybe a further rotation around the vertical axis providing that telluric and horizontal magnetic components are aligned with the geographic coordinate system or the strike. The absence of motion noise problems applies to stations m06–m11 that are situated off the continental slope in the trench and in the deep sea (Fig. 1b). The water depth is *ca.* 3800 m at site m06 and rises gently up to *ca.* 3100 m at site m11.

For the rest of the stations, there appear additional features in the tilt records that will be described in detail later. Roughly speaking, tilt motion and problems caused by it grow with the rise of the continental slope. Station m05 (depth: 3178 m) is affected by significant, but moderate motion noise still allowing for a standard processing. The motion noise of m04 in 1645 m depth is stronger: Its uncorrected and unselected data result in sounding curves that are not only very scattered, but not even similar to the curves obtained with motion noise taken into account. At station m03 in 1134 m depth relatively large tilt motion with a peculiar character is visible: Temporarily, tilt and magnetic data leave the range of the tiltmeter, or the data logger, respectively, and return to their initial values later on. Some selection is needed to avoid such out-of-range events in the data of this station during further processing. Station m02 placed in 162 m depth was lost, and the instrument of m01 situated in 87 m depth tilted over after a short time and did not yield meaningful data.

2.1.2 Direction relative to coast

Hence data of three stations (m03, m04 and m05) are suitable for tilt motion analysis and are considered further. The tilt is measured in two perpendicular components α_x and α_y per station that are aligned with the correspondent components of the magnetic sensor. Due to the deployment practice of marine instruments, the orientation of each station (i.e. of each α_x , α_y sensor pair) on the sea bottom relative to North (or to the coast line) is different. Now it can be observed that always one of the two tilt channels shows significantly larger motion amplitudes than the other. This is α_x for m03 and α_y for m04 and m05 (for the latter, see Fig. 2, both lowermost panels). It is striking that the dominant one coincides with the component directed more perpendicular to the coast according to the orientation of the given instrument.

2.1.3 Spectral distribution over time

The tilt time-series recorded at the three stations (see Fig. 2, lowermost panel, for m05) are characterized by the following features:

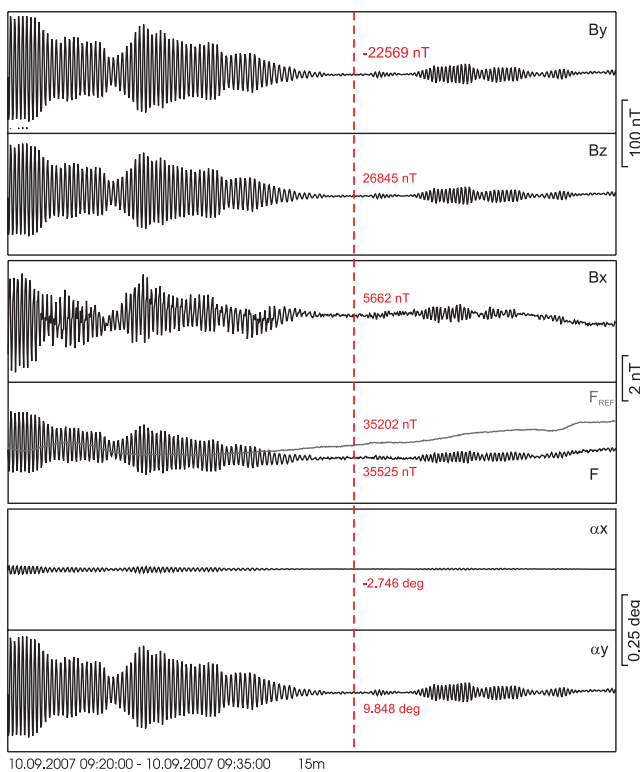


Figure 2. Time-series data of offshore station m05. Channels from top to down (in the instrument's coordinate system): magnetic components B_y , B_z , B_x , scalar total field F calculated from these and the same for the onshore reference site, tilt in x direction, tilt in y direction. Note that the vertical scale is different for each pair of panels and that the scale is not valid for the offset between both curves in the fourth panel. Representative static 'base' values for each channel are given along the vertical line. Obviously, the tilt in x direction is relatively quiet, the oscillating motion concentrates on the y direction. Highly correlated to this, there is a strong signal on magnetic y and z components, whereas B_x is hardly concerned. The fact that there are signals on F that are correlated to the y tilt, but are not present on the reference F , leads to doubts about the exactness of the total field measurement by the fluxgate magnetometer.

Superimposed on the static offset, prominent packages of harmonic oscillations with a period of 5–6 s and varying amplitudes are evident. The length and shape of such packages vary strongly. They can also be absent over a certain time interval. When considering low-pass filtered and condensed time-series, there are visible yet stronger, but not harmonic amplitudes occurring at a 6- and 12-h period. Fig. 3 summarizes the situation illustrating the α_x amplitude spectra of site m03 over a 10 d long time interval (the other stations would yield similar spectral distributions). Horizontal bright lines at 6 s, 6 and 12 h represent those maxima that can be found throughout the measurement. However, it is essential to note that the spectral content of the tilt record is not limited to these frequencies. In fact, over the whole frequency range relevant for magnetotellurics, some irregularly varying tilt motion is present, for example, at 100 s, its amplitude amounts to 0.1–0.5 arc minutes with some interruptions.

Lezaeta *et al.* (2005) do not mention tilt motion at larger periods, but they report similar quasi-harmonic oscillations with a maximum at 4.5 s. Interestingly, the length of the telluric tubes of the Woods Hole instruments is smaller, too, compared to that of the Geomar ones. It should be mentioned here that that maximum at *ca.* 6 s practically always occurs in measurements performed with the Geomar instruments, that is, in marine environments located in very differ-

ent places on the globe and also in data sets where motion noise is weak in general.

2.1.4 Interstation coherence

The last feature worthwhile mentioning is that the tilt motion is not coherent between different stations, even if the maxima mentioned above occur in the tilt records of each station. This can be seen in Fig. 4.

A plausible interpretation of all these findings could be the following: The tides (indicated by the 6- and 12-h cycle) cause a large-scale water streaming. The strength of the streaming component directed perpendicular to the coast grows with the rising of the continental slope. The streaming generates a swinging of the stations at a characteristic period of 5–6 s which is maybe comparable with the motion of a tree in the wind and is possibly smaller for measuring systems of smaller size. However, the physical details causing the beginning, amplitude and duration of this swinging seem to be locally different (possibly triggered by local bathymetry) and irregularly distributed in time. Hence, it appears impossible to explain these events more closely on the basis of tilt measurements alone. Lezaeta *et al.* (2005) could identify wind forces as source of the tilt motion they observed. Due to the deep-water environment considered here, this explanation should not be valid for our data set.

2.2 Effects of tilt motion on magnetic data

Fig. 2 shows raw time-series of magnetic and tilt channels for the Costa Rican offshore station m05, which are typical for the motion noise problems addressed here. It is immediately clear that the strong, high-frequency oscillations having periods between 5 and 6 s on B_y and B_z cannot have their origin in the natural variations of the Earth's electromagnetic field that usually are utilized in magnetotellurics. One would simply not expect variations with amplitudes of 100 nT in the dead band and beneath a 3-km-thick damping sea water layer.

Comparison with tilt components (both lowermost panels in Fig. 2) shows that there is a very high correlation between tilt motion and magnetic field variations. Especially for the dominating tilt direction α_y , the parallel magnetic component B_y and the 'vertical' magnetic component B_z (unprimed indices denote the coordinate system of the instrument's orientation on the seafloor here, which is not geographic or geomagnetic as tilt offsets as well as magnitude and sign of both 'horizontal' magnetic components B_x and B_y show), the character of variations in the time-series data is very similar. Fig. 4 confirms that coherence between a tilt channel and the parallel magnetic component is nearly perfect, also for longer periods and over many days as coefficients obtained from adjacent time windows were stacked to obtain these values.

The explanation for these variations supported also by Lezaeta *et al.* (2005) is the static main magnetic field of the Earth. Tilt motion indicates a swinging of the sensor such that the magnetic field is measured in a steadily changing coordinate system. For the given place and time the static field is approximately 35,320 nT according to the IGRF Model (<http://www.ngdc.noaa.gov/geomag-web/#igrfwmm>). Movements of, for example, 0.2° are transferred into variations of the magnetic components with amplitudes up to 120 nT (depending on the instrument's orientation with regard to the main field vector). Hence, these motion-induced magnetic variations are in the magnitude range of the natural

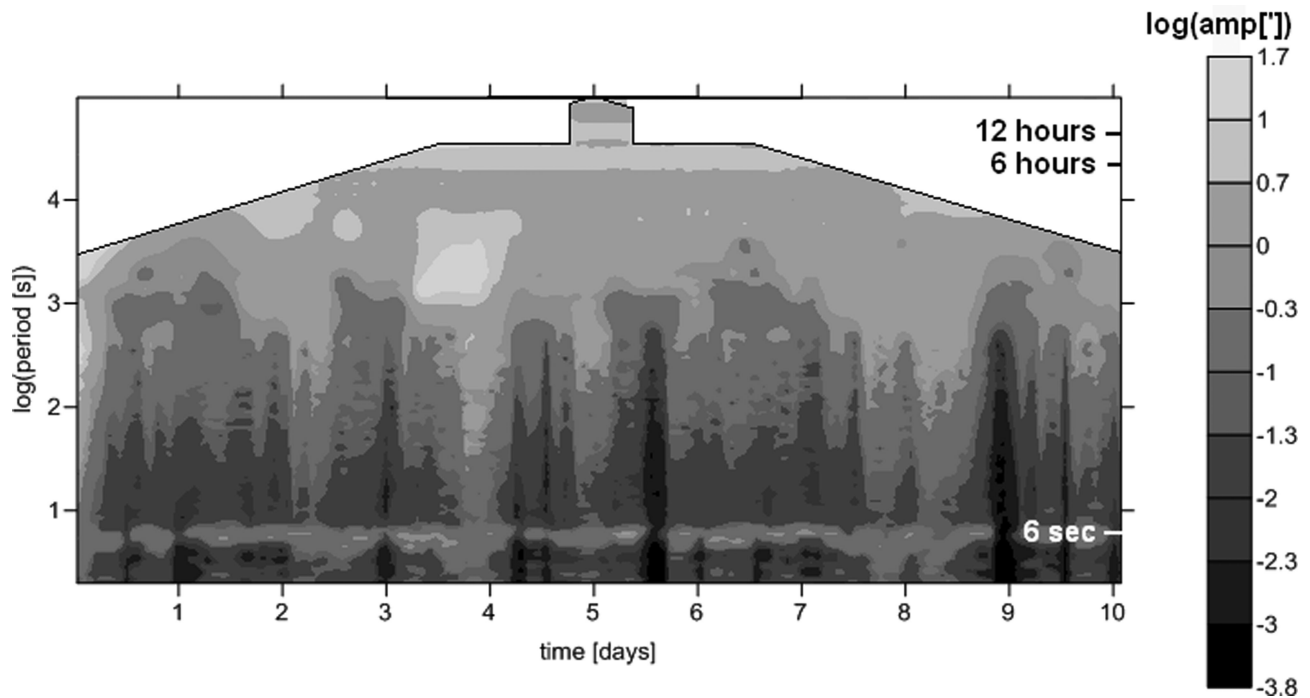


Figure 3. Distribution of tilt motion (α_y component of site m03) over period between November 8th and 18th. Throughout the measurement, there appear maxima at about 6 s, which remind the undulating variations visible on time-series (Fig. 2), and maxima at 12 and 6 h caused by the tides. However, a smaller tilt motion irregularly varying with time is present over the whole period range that is relevant for MT.

magnetic field variations which, unfortunately, almost vanish in that overwhelming tilt-correlated signal over the whole relevant period range. This is visible in the very small coherence between the magnetic field of the station under consideration and the onshore reference (Fig. 4). Under normal conditions, a high coherence close to 1 would be expected in magnetotellurics. Hence, data of the magnetic channels are heavily disturbed by motion noise.

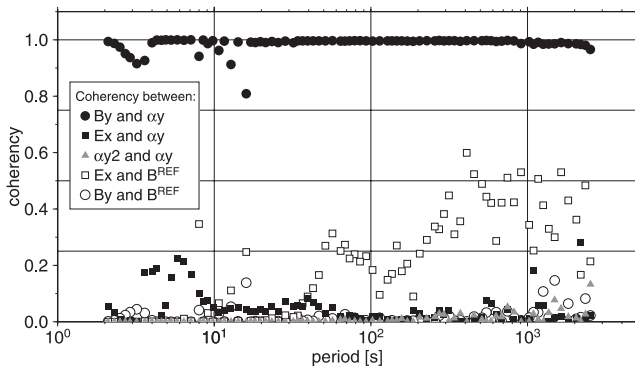


Figure 4. Coherence between several components of m05 and between these and those of other stations. Raw data in instruments' coordinates were used, but a rough alignment between different stations was given by incident. The numbers base on a 6-d-long time-series. We can see that: (1) Coherence between B_y and α_y is nearly perfect. (2) Coherence between E_x and α_y is clearly present, but only at short periods, and even there much weaker than that in (1). (3) Coherence between α_{y2} of station m04 and α_y is not present, that is, motion noise is not coherent interstationally. (4) Coherence between E_x and the roughly perpendicular horizontal magnetic component of the reference is too low for short periods, but clearly present at long periods. (5) Coherence between B_y and the roughly parallel reference component is not present.

2.3 Effects of tilt motion on telluric data

Motion noise is present on the electric channels, too. Fig. 5 shows the electric field components E_x and E_y at the same time as in Fig. 2 and a tilt-correlated signal is clearly visible. This complicates the situation with regard to processing for two reasons. First, it demonstrates that there exists noise correlated between the E and B fields of a station, that is, between input and output channels in terms of the processing. Correlated noise can lead to distorted transfer functions if there is no support by appropriate reference data. It is well known from onshore campaigns that the problem of correlated noise can be

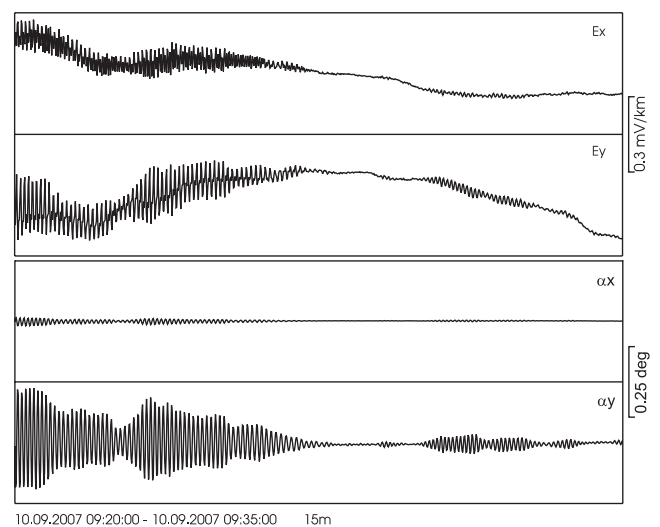


Figure 5. Telluric (upper panels) and tilt components (lower panels) of site m05 in the instrument's coordinate system for the same time as in Fig. 2. Telluric oscillations correlated to tilt motion in the 6s band are clearly visible, but less dominant than on magnetic channels.

severe for magnetotellurics, where the underlying disturbances are often caused by DC railways (e.g. Larsen *et al.* 1996; Pádua *et al.* 2002; Ernst *et al.* 2008).

The second problem about the telluric motion noise is that the way it is physically generated is very different from the explanation for the magnetic noise, since there is no static electric field on the seafloor. In fact, the source of electric motion noise is a fundamental law of electromagnetics: A closer look at the telluric time-series in Fig. 5 shows that this noise is not as huge and overwhelming as for the magnetic channels. More precisely, there is visible a long-period variation that has no counterpart in the tilt channels, so it is probably of natural origin and features relevant for magnetotellurics are discernible. A glance at coherencies in Fig. 4 confirms this: First, coherence between α_x and the perpendicular E_x is only about 0.2, and even this holds only for short periods up to about 8 s, whereas it descends into meaninglessness at longer periods. In contrast, the coherence between E_x and the (more or less) perpendicular horizontal magnetic component of the reference station is close to zero at short periods, but becomes relevant at *ca.* 1 min, and rises up to 0.6 at several hundred seconds. This is almost what one would expect in magnetotellurics and definitely better than the magnetic coherence to the reference.

So we have the finding that the relationship between tilt and telluric data is better defined for high frequencies than for low frequencies. This can be a hint that the electric field does not depend on the tilt directly, but on its rate of changing, or time derivative, respectively, since high frequencies are equivalent to more rapid, that is, larger changes. Bearing in mind the perfect coherence between tilt and magnetic field, one could also say: The electric field depends on the time derivative of the magnetic field. This is the well-known principle of electromagnetics called Faraday's law and expressed in one of Maxwell's equations,

$$\text{rot}(\vec{E}) = -\frac{d\vec{B}}{dt}. \quad (1)$$

It is our hypothesis that this equation connects the motion noise in the electric and in the magnetic field, or that the motion noise on telluric channels is induced by that on the magnetic channels. Note that this 'induction due to tilt motion' takes place only in the swinging instrument and has to be distinguished from induction in the solid Earth that is the base for the magnetotelluric method.

Eq. (1) is difficult to verify since magnetotelluric data do not allow for a determination of $\text{rot}(\vec{E})$. Hence, we try to prove the induction phenomenon for our data in the following simplified form: A particle carrying the electric charge q moving with the instantaneous velocity \vec{v} perpendicular to the field lines of a homogeneous magnetic field of induction \vec{B} experiences the Lorentz force \vec{f}_L that is acting perpendicular to both its motion's and the magnetic field's directions,

$$\vec{f}_L = q\vec{v} \times \vec{B}. \quad (2)$$

In the frame of reference of the particle, this force is recognized as electric field \vec{E} ,

$$\vec{E} = \vec{v} \times \vec{B}. \quad (3)$$

In a first approximation, the tilt motion takes place in vertical direction. Hence, it is perpendicular to the horizontal component \vec{H} of the Earth's main magnetic field. The value of \vec{H} in the measurement area is about 28 000 nT = 2.8×10^{-5} Vs m⁻².

We consider the tilt motion maximum in the dead band first, which amounts to about 5 arc min at a period of *ca.* 6 s (*cf.* Fig. 2, lowermost panel). This corresponds to the amplitude $A_0 \approx 7 \times$

10^{-3} m at the tube ends if we take into account that the half length of the telluric tubes is 5.1 m. Assuming now that the tilt motion can be roughly described by a harmonic oscillation, the velocity of a tube end when passing the zero-point position is

$$\vec{v} = A_0\omega = 7 \times 10^{-3} \text{ m} \times 2\pi/6\text{s} \approx 7 \times 10^{-3} \text{ m s}^{-1}. \quad (4)$$

This velocity has to be multiplied by 2 since both ends of a tube move in opposite directions. Hence, according to eq. (3), we obtain the electric field

$$\vec{E} = 2 \times 7 \times 10^{-3} \frac{\text{m}}{\text{s}} \times 2.8 \times 10^{-5} \frac{\text{Vs}}{\text{m}^2} \approx 4 \times 10^{-7} \frac{\text{V}}{\text{m}} = 0.4 \frac{\text{mV}}{\text{km}}. \quad (5)$$

This is roughly the electric field that would be induced in a telluric tube oriented perpendicular to \vec{H} , that is, more or less in E-W direction (whereas no induction takes place in a tube directed parallel to \vec{H}). This value will be split up vectorially between the E_x and E_y channels depending on the orientation of the instrument. It is obvious that such an electric field value as in eq. (5) cannot be neglected in the context of our measurements and that it is in the order of magnitude of the telluric motion noise that we observe, *cf.* Fig. 5.

However, if we repeat this consideration for the much slower tilt motion connected with the tides, we get (in spite of its larger amplitudes) electric field values smaller than 10^{-3} mV km⁻¹ that are meaningless for our measurements. Hence, the idea that telluric motion noise is caused by simple electromagnetic induction appears plausible.

Lezaeta *et al.* (2005) also consider this idea of motion-noise generation on electric channels. They regard it as improbable for their data, but they do not come to a final explanation for this type of noise.

3 TWO METHODS FOR MOTION-NOISE REDUCTION IN MAGNETIC TIME-SERIES

Dynamic tilt records allow for a prediction and correction of magnetic motion noise in a certain degree as will be shown in this section. However, it should be kept in mind that a general limitation might exist for the success of such attempts: For a complete description of a motion or change of orientation measurements of three angles are necessary. The data set used provides only information on the current inclination between the sensor's *XY* plane and the true horizontal plane, whereas information on a possible changing of the twist around the instrument's vertical axis is missing. In both approaches presented in the following we consequently need to assume that this angle is constant.

3.1 The point-to-point re-rotation

The point-to-point re-rotation requires not only dynamic tilt records in the data set, but also the full vector of the magnetic field including the static main part. This requirement is different than in onshore magnetotellurics and not met in all types of offshore instruments either. It means that this correction method is applicable only on data collected by fluxgate magnetometer systems. This instrument type is able to measure not only the three components of magnetic field variations, but also of the total field vector. In onshore magnetotellurics this ability of fluxgates is used to orient the magnetic sensor to North before the recording. Then the static field part is

compensated away and only the variations are recorded. If fluxgates are applied in offshore measurements, the total field is recorded at least for some time. It is used to determine the orientation of the sensor *a posteriori*. This is done by finding the angle to the geomagnetic North direction (which minimizes B_y and maximizes B_x) after levelling the magnetic measurement according to the tilt values. If, for example, induction coil magnetometers are used the information on the sensor's orientation must be provided by a compass. As long as the rotation angles are constant for the whole time-series the operations for levelling and North-aligning can be performed on the components of magnetic variations alone and the total field vector is not necessary.

The idea of the point-to-point re-rotation is that every single data sample of the full magnetic field vector $(B_x, B_y, B_z)^T$ is levelled separately according to the correspondent tilt samples. Thereby the motion-induced noise on magnetic channels is compensated. Thus it is a coordinate transform from the swinging coordinate system in which the instrument measures to a fixed coordinate system before the North-aligning. Such approaches are published in Fitterman & Yin (2004), who use Euler's angles to perform that operation, and in Nowożyński (2005), who formulates it in a somewhat different way but yields the same result. We use the implementation of the latter here. For details of these operation, the reader is referred to that literature.

The result of the application of the point-to-point re-rotation to the data displayed in Fig. 2 can be seen in Fig. 6. The tilt-correlated variations have not vanished, but they have been reduced dramatically by a factor of *ca.* 20. It can be shown that the reason for this not ideal result lies not in the method, but in the data: Calculating the scalar value of the total field F according to

$$F = \sqrt{B_x^2 + B_y^2 + B_z^2}, \quad (6)$$

for each sample should result in a time-series that is not correlated with the tilt series, since F is by definition independent of coordinate system, rotation, or orientation. However, the plot in the fourth panel

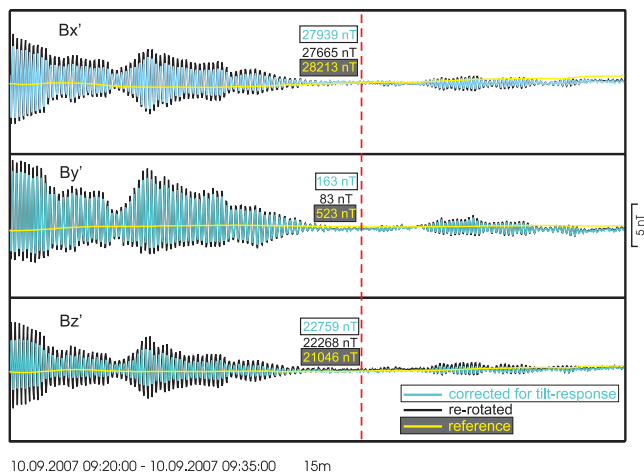


Figure 6. Time-series of magnetic components of station m05 after correction by point-to-point re-rotation (black) and for tilt-response (turquoise in electronic version, grey in printed version) in geomagnetic coordinates. Time-series of the reference are given in yellow (white in printed version) colour for comparison. Note that the vertical scale is not valid for offsets between different time-series, their true values are given at the vertical line instead. The motion-induced oscillations do not vanish completely, but they are reduced by a factor of *ca.* 20 as comparison with Fig. 2 shows. Results after both methods are very similar, where the tilt-response correction leads to slightly smaller oscillations, especially for the B_z component.

of Fig. 2 shows that this is not the case, the tilt-correlated oscillations are striking, even if their amplitudes of *ca.* 1 nT are small. We have many hints on some inaccuracy in the main field measurement of this data set which would explain this phenomenon. This topic is discussed in Appendix A.

3.2 The tilt-response correction

The tilt-response correction developed in this paper is a new alternative to the point-to-point re-rotation in terms of motion-noise reduction in magnetic time-series. It has a clear advantage in comparison to the method described before: it does not require information on the total field at all. In fact, it provides such information. Therefore, it can be applied to marine MT data measured with induction coil systems or torsion photoelectric magnetometers as well as to those measured by means of fluxgate instruments, provided that dynamic tilt records are available. A certain disadvantage of the tilt-response correction is that it is an approximation. Hence, its principal accuracy is largest for signals of small amplitudes and decreases with increasing variation amplitudes, whereas the point-to-point re-rotation is an exact method.

3.2.1 Method and result

The tilt-response correction can be derived from the point-to-point re-rotation utilizing some simplifications and linear approximations. This is outlined in Appendix B. However, it is also instructive to introduce it in another way: The obviously perfect correlation between tilt components on the one hand and the magnetic field variations on the other hand illustrated in Figs 2 and 4 suggests a proceeding that is formally analogous to transfer function estimation:

In every-day magnetotellurics horizontal magnetic components of a station (input channels) are used to explain its telluric ones (output channels) via the impedance (transfer function). Here, it seems worthwhile trying to explain a station's magnetic field (acting as output channels) by the tilt measurements (regarded as input channels) in a similar way via a simple linear relationship in the frequency domain. More detailed, the measured magnetic field $\vec{B} = (B_x, B_y, B_z)^T$ of a station in the instrument's coordinate system is regarded as a superposition of the following signals: A part $\vec{B}^{\text{INDUCTION}}$ which is relevant for magnetotellurics and coherent with the horizontal magnetic components of the onshore reference station (in geomagnetic coordinates denoted by primes) \vec{B}^{REF} , a second part \vec{B}^{MOTION} that is caused by motion and coherent with the tilt channels $(\alpha_x, \alpha_y)^T$ and a third part \vec{B}^{UN} that cannot be correlated to anything, that is,

$$\vec{B}(\omega) = \vec{B}^{\text{INDUCTION}}(\omega) + \vec{B}^{\text{MOTION}}(\omega) + \vec{B}^{\text{UN}}(\omega) \quad (7)$$

or

$$\begin{pmatrix} B_x \\ B_y \\ B_z \end{pmatrix} = \begin{pmatrix} M_{xx'} & M_{xy'} \\ M_{yx'} & M_{yy'} \\ M_{zx'} & M_{zy'} \end{pmatrix} \begin{pmatrix} B_{x'} \\ B_{y'} \end{pmatrix}^{\text{REF}} + \begin{pmatrix} \text{TRF}_{xx} & \text{TRF}_{xy} \\ \text{TRF}_{yx} & \text{TRF}_{yy} \\ \text{TRF}_{zx} & \text{TRF}_{zy} \end{pmatrix} \begin{pmatrix} \alpha_x \\ \alpha_y \end{pmatrix} + \begin{pmatrix} B_x \\ B_y \\ B_z \end{pmatrix}^{\text{UN}}. \quad (8)$$

The tensor \mathbf{M} corresponds (except for the last line) to the Horizontal Magnetic Tensor or inter-station transfer function between local and remote site known from the magnetovariational sounding method

(e.g. Schmucker 1970; Soyer & Brasse 2001; Habibian *et al.* 2010). It is, however, twisted due to the different coordinate systems of both instruments. TRF is the tensor of the station's magnetic tilt-response function.

The least-square solution for both transfer functions is estimated under the condition that \vec{B}^{UN} becomes minimum for a large number N of all data coefficients, that is, with the symbols for output and input channels

$$\mathbf{OUT} = \begin{pmatrix} B_{x1} & B_{y1} & B_{z1} \\ \vdots & \vdots & \vdots \\ B_{xN} & B_{yN} & B_{zN} \end{pmatrix}, \quad (9)$$

$$\mathbf{IN} = \begin{pmatrix} B_{x'1}^{\text{REF}} & B_{y'1}^{\text{REF}} & \alpha_{x1} & \alpha_{y1} \\ \vdots & \vdots & \vdots & \vdots \\ B_{x'N}^{\text{REF}} & B_{y'N}^{\text{REF}} & \alpha_{xN} & \alpha_{yN} \end{pmatrix}, \quad (10)$$

and for the transfer functions

$$\mathbf{F} = \begin{pmatrix} M_{xx'} & M_{xy'} & \text{TRF}_{xx} & \text{TRF}_{xy} \\ M_{yx'} & M_{yy'} & \text{TRF}_{yx} & \text{TRF}_{yy} \\ M_{zx'} & M_{zy'} & \text{TRF}_{zx} & \text{TRF}_{zy} \end{pmatrix}, \quad (11)$$

we obtain

$$\mathbf{F}^T = (\mathbf{IN}^\dagger \mathbf{IN})^{-1} \mathbf{IN}^\dagger \mathbf{OUT}, \quad (12)$$

where an upper index T denotes the transpose matrix and a \dagger the Hermitian transpose.

Obviously, this approach differs from the usual magnetotelluric ones by the number of input channels in \mathbf{IN} and the number of transfer function components in \mathbf{F} . Although there is just one pair of input channels in both the usual single-site and the usual remote-reference equation, here appears another pair (the tilt components) that leads to the additional TRF transfer functions. However, there is one magnetotelluric processing approach that is formally very similar. It is the signal–noise separation by Larsen *et al.* (1996). This method is also based on four input channels from which one pair leads to MT transfer functions and the other one refers to correlated noise.

The induction part (\mathbf{M}) of the transfer function obtained by this estimation is not included in the further procedure for two reasons: First, because there are, as mentioned, complications due to an implicit coordinate transform, and second, as a least-square solution, this result is naturally inferior compared to robust transfer function estimations. Instead, the TRF is used to reconstruct the motion-noise part of the magnetic data now:

$$\begin{pmatrix} B_x \\ B_y \\ B_z \end{pmatrix}^{\text{MOTION}} = \begin{pmatrix} \text{TRF}_{xx} & \text{TRF}_{xy} \\ \text{TRF}_{yx} & \text{TRF}_{yy} \\ \text{TRF}_{zx} & \text{TRF}_{zy} \end{pmatrix} \begin{pmatrix} \alpha_x \\ \alpha_y \end{pmatrix}. \quad (13)$$

Subtracting this reconstructed motion noise from the original data leads to magnetic data corrected for motion noise,

$$\vec{B}^{\text{CORRECTED}}(\omega) = \vec{B}(\omega) - \vec{B}^{\text{MOTION}}(\omega). \quad (14)$$

Having done this for the coefficients of all available frequencies, we can transform them back into time domain and obtain time-series that are (after levelling) ready for processing with an established code like usual onshore MT data.

Corrected time-series are shown in Fig. 6. The noise reduction result is slightly better than that by the point-to-point re-rotation, but the difference is very small.

3.2.2 Properties and meaning of the tilt-response function

In Section 3.2.1, we have shown how to correct the magnetic time-series for the tilt-response. So the main goal of the method has been reached. However, it turned out that the tilt-response function is more than a means to reduce motion noise. In fact, it provides information on the total magnetic field. We want to outline this in the following.

Due to the way it is defined and estimated, the TRF is formally a complex-valued function of frequency like other transfer functions in magnetotellurics and related methods (e.g. impedances or inter-station transfer functions). Thus we display it as modulus and phase. Now it turned out that some of its components are more stable than others. This means that they are constant over frequency or period, respectively, hardly scattering, have small error bars and phases about either 0 or $\pm 180^\circ$. Obviously, we are dealing more with a constant, real-valued factor of proportionality than with a frequency-dependent, complex-valued transfer function. Moreover, it is predictable *a priori* which components will have these properties: it is either TRF_{xx} or TRF_{yy} , depending on which tilt channel has the dominant signal (for the case shown in Fig. 2, it is TRF_{yy} , *cf.* Fig. 7), and both ones connected to the vertical magnetic component (TRF_{zx} , TRF_{zy}) where, again, that one referring to the dominant tilt component is more stable (Fig. 7). The reason for the lower quality of the TRF curves depending on channel α_x is probably that typical α_x amplitudes hardly exceed the warranted resolution of the tiltmeter which amounts to 0.01° (*cf.* Fig. 2). The rest of the ‘horizontal’ components is (if at all) stable only over a small period range and in such cases, the second ‘main diagonal’ component shows a tendency to the same modulus as the first one, whereas the modulus of the ‘off-diagonal’ ones is much smaller. These features always result under the same conditions, for example, for different time-series fragments of the same station.

It is reasonable to expect that such reliably reproducible properties of the TRF have their origin in the nature of the relationship between changes in the tilt and the magnetic field components. To understand this, we consider a simplified model of what happens to the magnetic field vector under tilt motion: We neglect natural variations of the magnetic field, that is, all field variations are due to the oscillating coordinate system. The magnetic field shall have only the vertical (Z) and one horizontal (H) component, and there is only motion correspondent to one tilt component α that is parallel to H (Fig. 8). If the tilt were 0, we would measure H_0 and Z_0 in a quasi-onshore manner. If the instrument stands inclined such that some static tilt is involved, H_0 and Z_0 refer to the instrument's coordinate system instead. With a dynamic tilt α differing from 0, we measure the components $H(\alpha)$ and $Z(\alpha)$ that are related to H_0 and Z_0 via a simple rotation by the angle α ,

$$\begin{pmatrix} H(\alpha) \\ Z(\alpha) \end{pmatrix} = \begin{pmatrix} \cos(\alpha) & \sin(\alpha) \\ -\sin(\alpha) & \cos(\alpha) \end{pmatrix} \begin{pmatrix} H_0 \\ Z_0 \end{pmatrix}. \quad (15)$$

The rotation is in clockwise direction according to the convention applied in our measurements.

Taking into account that the variations of α are very small, that is, in the range of arc minutes (*cf.* Fig. 3), it is suggestive to substitute $\sin(\alpha)$ by α and $\cos(\alpha)$ by 1. The resulting linear relationships are

$$H(\alpha) \approx Z_0 \alpha + H_0, \quad (16)$$

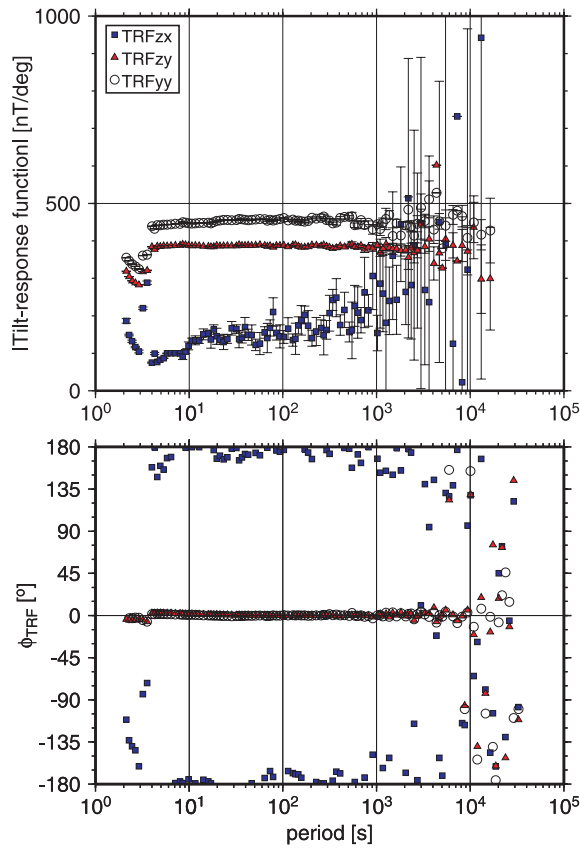


Figure 7. Modulus (top) and phase (bottom) of selected tilt-response functions of site m05. It is evident that, especially in case of TRFs of the stronger oscillating y tilt channel (i.e. TRF_{yy} and TRF_{zy}), the functions are very stable and constant over period. Phases are either 0 (TRF_{zy} , TRF_{yy}) or 180 (TRF_{zx}) degree. This means that the relationship between tilt and its magnetic response is rather a real-valued factor of proportionality than a complex transfer function.

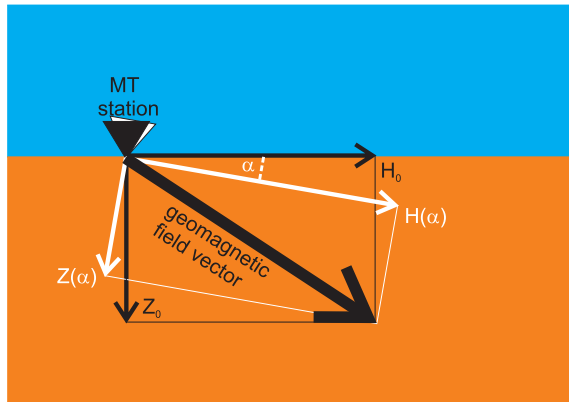


Figure 8. Simplified demonstration of the dependency of the the measured magnetic components on the tilt. Beside of the vertical component Z , we consider only one horizontal component H and one (the corresponding) tilt direction α . If the tilt were zero, the instrument would split up the geomagnetic field vector into the ‘true’ geomagnetic components H_0 and Z_0 (black arrows). The change of this splitting occurring in the case of non-zero α and resulting in the components $H(\alpha)$ and $Z(\alpha)$ (white arrows) has the character of a simple rotation by the tilt angle α .

$$Z(\alpha) \approx -H_0\alpha + Z_0. \quad (17)$$

Hence, the proportionality factor between magnetic field component and tilt is Z_0 for $H(\alpha)$ and $-H_0$ for $Z(\alpha)$. Assuming now that more complicated interdependencies due to the third magnetic and the second tilt component can be neglected, we can substitute $H(\alpha)$, H_0 , α by either B_x, X_0, α_x (case A) or B_y, Y_0, α_y (case B) and $Z(\alpha)$ by B_z . Identifying the factors of proportionality with the corresponding tilt-response function elements (*cf.* the motion part of eq. 8) leads to the assignments

$$\text{TRF}_{xx} \approx Z_0, \quad (18)$$

$$\text{TRF}_{zx} \approx -X_0 \quad (19)$$

from case A and

$$\text{TRF}_{yy} \approx Z_0, \quad (20)$$

$$\text{TRF}_{zy} \approx -Y_0 \quad (21)$$

from case B.

X_0, Y_0 and Z_0 are the static (or mean) values of the total magnetic field components in the instrument’s coordinate system. Since these have been measured by the fluxgate magnetometer, it is obvious how to check this result, this will be done in the next Section 3.2.3. However, it is immediately visible that it meets some general properties of the TRF components, for example, being a simple real value, the equality of the TRF_{xx} and the TRF_{yy} elements and the practically missing TRF_{xy} and TRF_{yx} elements.

For practical application in terms of motion noise removal it has been found useful to simplify the TRF functions estimated via eq. (12). This means to substitute the whole function by one selected, obviously well-estimated value of it for the reconstruction of the tilt response. Such a step has three advantages: First, modulus (and phase) of the function can be down-biased (or scattered, resp.) due to weak signals or instrumental noise on the tilt channels (or non-motion noise on the magnetic channels, resp.) in some period range. By selecting the value at an obviously well-estimated period and taking it for the whole range distortions during the reconstruction can be avoided. Second, the frequency range of the estimated transfer function is limited: The longest period where reasonable TRF values can be estimated is much shorter than the longest period (corresponding to the whole time-series length) where coefficients for the tilt series are available. So a precise usage of the transfer function in eq. (13) would mean to limit the reconstructed time-series to the frequency range of the transfer function, that is, to apply a high-pass filter. This problem can be avoided by using the constant factors which are known to be valid for the whole frequency range. Third, such a full-range application of eq. (13) on the tilt time-series leads (after subtraction of the result from the original magnetic ones) to noise-corrected time-series that are already levelled. Otherwise an extra operation would have to be performed to align the instrument’s B_z axis with the true vertical axis.

Data are ready for processing after subtraction of the reconstructed tilt response from the raw magnetic time-series (eq. 14), where the reconstruction is performed according to eq. (13) with the matrix modified as follows:

$$\mathbf{TRF}^{\text{mod}} = \begin{pmatrix} (\pm\text{TRF}_{jj}, 0) & (0, 0) \\ (0, 0) & (\pm\text{TRF}_{jj}) \\ (\pm\text{TRF}_{zx}) & (\pm\text{TRF}_{zy}) \end{pmatrix} (\omega_{\text{selected}}), \quad (22)$$

where the index j stands for x or y depending on which tilt channel has the stronger signal, and the real parts of each element have a

Table 1. Comparison of total field components (in the instrument's coordinate system) measured by fluxgate magnetometer and according to the tilt-response function.

Station	Component	After fluxgate (nT)	After TRF (nT)
m03	X_0	$-27\,621 \pm 188$	$-26\,929 \pm 252$
	Y_0	$15\,984 \pm 63$	$15\,470 \pm 82$
	Z_0	$15\,289 \pm 297$	$13\,178 \pm 22$
m04	X_0	5806 ± 39	4584 ± 23
	Y_0	$28\,308 \pm 166$	$27\,788 \pm 6$
	Z_0	$20\,375 \pm 235$	$19\,194 \pm 17$
m05	X_0	5483 ± 10	5730 ± 45
	Y_0	$-22\,875 \pm 48$	$-22\,220 \pm 10$
	Z_0	$26\,571 \pm 39$	$25\,700 \pm 25$

positive sign in case of a 0 phase of the correspondent calculated TRF element and a minus sign if the phase is $+180^\circ$ or -180° . The time-series corrected for tilt-response that are displayed in Fig. 6 have been obtained by means of a TRF modified in the described way.

3.2.3 Comparison of measured and derived total field components

Here it shall be checked if the interpretation that the tilt-response functions reflect mainly the main field components is reasonable. We possess values for the main field components measured directly with the fluxgate magnetometer. Hence a comparison of values from both 'sources' is straightforward.

The standard deviation of the TRF estimation at the selected period can be regarded as a measure of the method's accuracy, it will reflect the stability of the underlying transfer function. For the fluxgate measurement it appears reasonable to take the average value of the magnetic component's time-series that has been used for the TRF estimation before, and to take the RMS deviation of the time-series as its accuracy. The latter is, of course, inspired by the idea that the variations limit the exactness of the mean value which is also visible for the other method. It does not mean that we have such an expectation of accuracy to a concrete, single fluxgate measurement. Such a measurement should be much better if we assume a careful calibration.

Table 1 lists the main field components in the instrument's coordinate system after both methods. It is clear that the results of both methods are similar. However, taking into account their estimated accuracy there must be stated that they do not agree. The differences are significant with values between 200 and 2000 nT, and for all stations, they are maximum on the Z_0 component.

4 PROCESSING AND SOUNDING CURVE RESULTS

After correction of magnetic data as presented in Sections 3.1 and 3.2, data are ready for a standard robust processing, where telluric data remain unchanged. Raw data are processed, too, for comparison. We used Egbert's code (Egbert & Booker 1986) including the remote reference technique. Reference is an onshore magnetic station without data quality problems.

Sounding curves of stations m03, m04 and m05 are shown in Figs 9–11. They were rotated into the strike direction of -55° (i.e. roughly along the Pacific coast) that has been taken from Worzewski *et al.* (2011). TE modes are characterized by features unknown in

an onshore context, that is, a sharp maximum in the ρ_a curves and a phase wandering through almost all quadrants over period. These features are, roughly speaking, explained by the coast effect from the perspective of the seafloor as reported in Worzewski *et al.* (2012). Sounding curves after both correction methods agree with the results presented by Worzewski *et al.* (2011) and Worzewski (2011) that were obtained by means of the BIRRP code (Chave & Thomson 2004) from selected quiet sections. However, the transfer function quality could be significantly improved here insofar as their range has been extended to both short and long periods, and the curves have become more continuous.

In all figures from 9 to 11, there is an obvious improvement from raw data (a) to corrected data (b,c). Especially Figs 9 and 11 show that the sounding curves become more continuous to longer periods due to correction. The observation that a noise-cleaning of time-series improves the remote reference result mainly at longer periods is also reported by Kappler (2012) in a more general context. The partly rather large error bars in the data-corrected curves represent the abundant remains of the motion noise, which, however, the robust remote reference code copes very well with. Differences between (b) and (c), that is, between results after both time-series correction methods, are small in general, and it is difficult to say which result to prefer for the further modeling work. An exception is m03 (Fig. 9), where a slight systematic deviation is visible in the TE mode. Since m03 is the station with the largest motion amplitudes (*cf.* Section 2.1), a possible reason for this problem could be that the limitations due to the approximations used in the tilt-response method are overstretched already. Hence, it seems more conservative to prefer the sounding curves after the point-to-point re-rotation in this case.

5 SUMMARY AND CONCLUSIONS

A marine data set from Costa Rica has been investigated in terms of motion noise. This was possible due to tilt records sampled with the same rate as the magnetotelluric channels at each station, and it was necessary because motion noise is extraordinary strong for some stations and does not allow for a standard processing.

The analysis of the tilt motion itself revealed features obviously connected to the tides, an amplitude maximum in the dead band and smaller but relevant, irregularly distributed signatures in the whole frequency range in-between. Although details of the generation of that motion must remain speculative, its effects on magnetic and telluric data could be explained quite unambiguously: The magnetic motion noise consists of variations resulting from the main field of the Earth that is measured in a swinging coordinate system if tilt motion is present. It affects the whole frequency range like the tilt motion itself. The motion noise on telluric channels is generated via electromagnetic induction due to the motion of the instrument in the static main magnetic field, and it is much weaker for low frequencies than for the high-frequency range. Motion noise is not coherent between channels of different stations.

The knowledge that motion noise is (a) practically absent in the telluric data at longer periods and (b) is weaker on telluric than on magnetic channels can be very beneficial for the processing. It can be applied if magnetic time-series cannot be corrected for motion noise, for example, because dynamic tilt records are unavailable. In such cases processing techniques that regard the horizontal magnetic components as noise-free input channels should not be applied. Instead, approaches can be recommended where either telluric channels act as input (i.e. utilizing the admittance and,

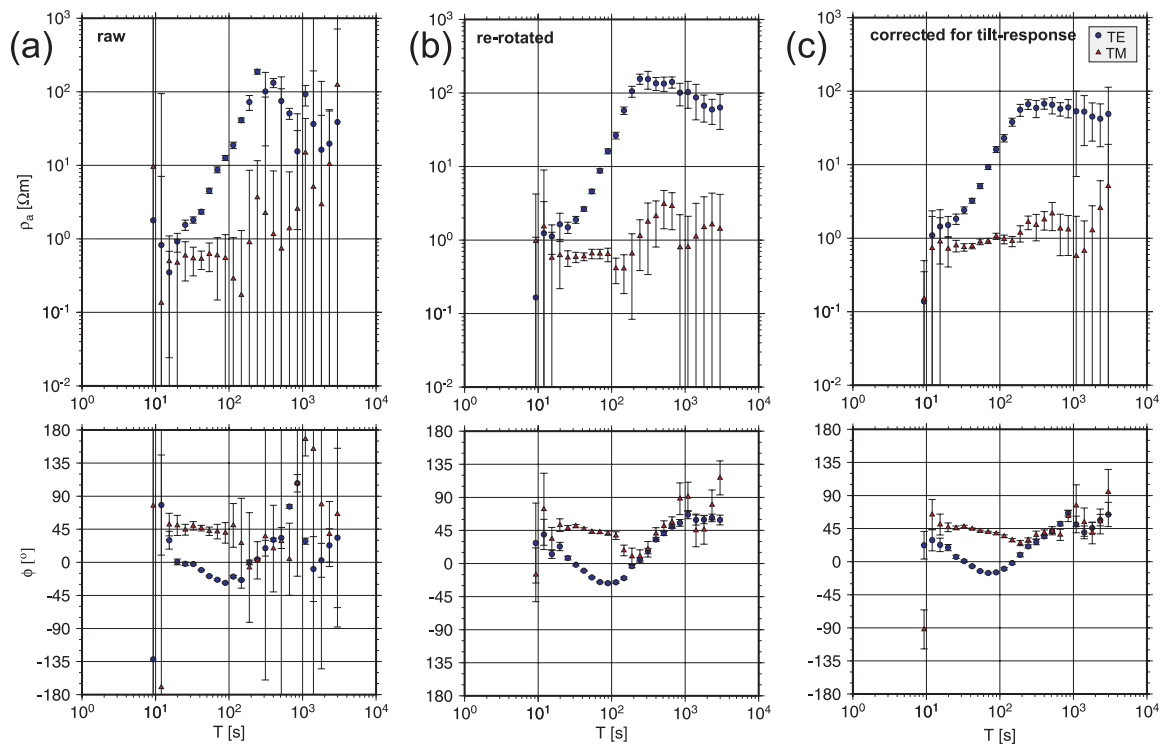


Figure 9. Sounding curves for site m03 (rotated to strike) after different time-series preparations. 4 pieces of time-series (length: 6 d each) were used. Selection was necessary because data were temporarily out of range. (a) Raw data, (b) magnetic time-series point-to-point re-rotated and (c) magnetic time-series corrected for tilt-response.

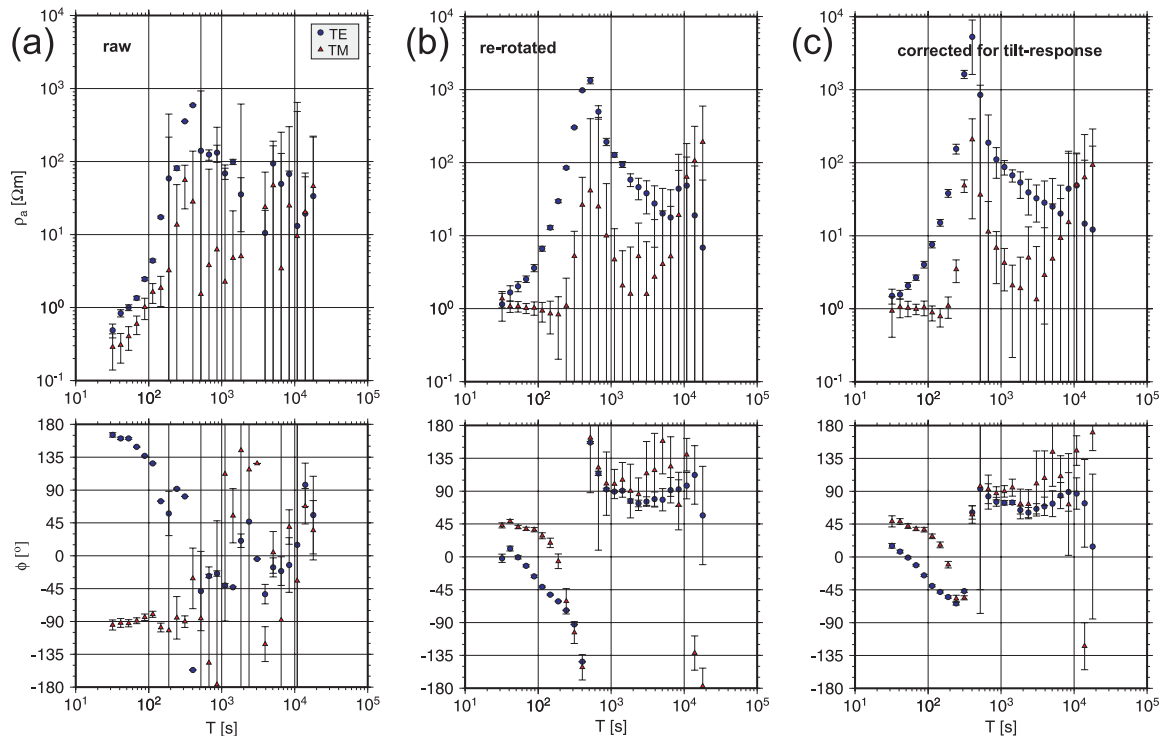


Figure 10. Sounding curves for site m04 (rotated to strike) after different time-series preparations. Length of time-series used 48 d. (a) Raw data, (b) magnetic time-series point-to-point re-rotated and (c) magnetic time-series corrected for tilt-response.

if onshore reference stations are unavailable, using telluric channels as reference data) or where principal component analysis is applied as in the multiple-station processing by Egbert (1997). The latter has the additional advantage that its suitability for synchronous data

of many stations matches the deployment practice of marine arrays. The capability of the recommended approaches it not demonstrated here, but it is confirmed by experiences gained from other marine data sets.

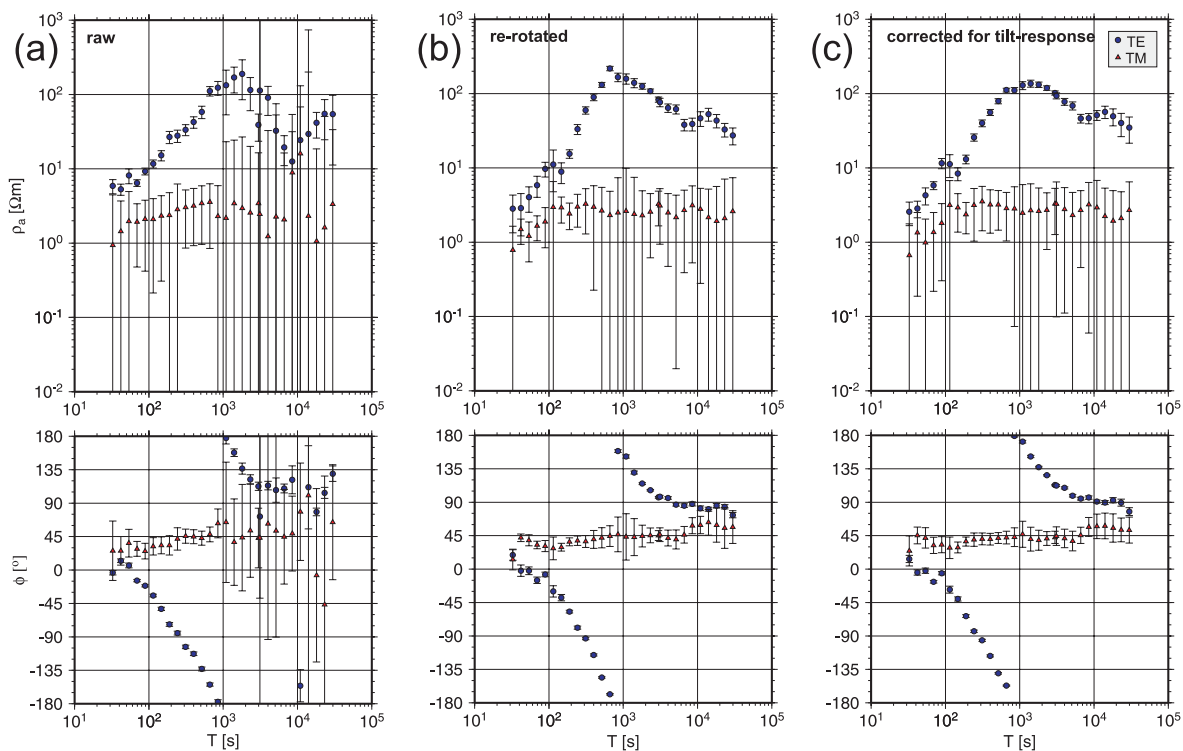


Figure 11. Sounding curves for site m05 (rotated to strike) after different time-series preparations. Length of time-series used 48 d. (a) Raw data, (b) magnetic time-series point-to-point re-rotated and (c) magnetic time-series corrected for tilt-response.

With tilt records at hand, magnetic time-series data have been corrected for motion noise. The first method for this, a coordinate transform, produced results that are good, but less exact than expected. We have many hints that the reason for this is lacking accuracy in the fluxgate magnetometer measurement of the main field. A new correction approach for motion noise called tilt-response correction does, in contrast to the first one, not require a total field measurement. It reduced the motion noise somewhat better and additionally, provides an alternative source of information about the Earth's total magnetic field. Magnetic time-series corrected by either method resulted in very similar and good-quality sounding curves after the processing.

To overcome motion noise problems in marine magnetotelluric data, a usage of dynamic tilt records can be recommended. If the tilt-response correction is applied then, measurements reliant on other than fluxgate-type magnetometers should benefit from it as well.

ACKNOWLEDGEMENTS

We thank Tamara Worzewski for her openness and responsiveness that decisively supported the development of this study. Contributions of Paweł Czubak and Michał Sawicki to the experimental work on dry ground are acknowledged, and we owe an important hint on electromagnetic fundamentals to the latter. Several valuable hints came from Heinrich Brasse. We thank Leonid Rakhlin, Olaf Hillenmaier, Hans-Ulrich Auster, Herrmann Lühr and Patricia Ritter for valuable insights into the world of both fluxgate magnetometer manufacturers and their users for main field measurements. We are grateful to Xavier Garcia and an anonymous reviewer for many comments leading to improvements in the manuscript. The data analysed here have been measured in the framework of the project

SFB574 'Volatile and Fluids in Subduction Zones' funded by the Deutsche Forschungsgemeinschaft.

REFERENCES

- Chave, A.D. & Thomson, D.J., 2004. Bounded influence magnetotelluric response function estimation, *Geophys. J. Int.*, **157**, 988–1006.
- Egbert, G.D., 1997. Robust multiple-station magnetotelluric data processing, *Geophys. J. Int.*, **130**, 475–496.
- Egbert, G.D. & Booker, J.R., 1986. Robust estimation of geomagnetic transfer functions, *Geophys. J. R. astr. Soc.*, **87**, 173–194.
- Ernst, T. *et al.*, 2008. Electromagnetic images of the deep structure of the Trans-European Suture Zone beneath Polish Pomerania, *Geophys. Res. Lett.*, **35**, doi:10.1029/2008GL034610.
- Fitterman, D.V. & Yin, C., 2004. Effect of bird maneuver on frequency-domain helicopter EM response, *Geophysics*, **69**(5), 1203–1215.
- Habibian, B.D., Brasse, H., Oskooi, B., Ernst, T., Sokolova, E. & Varentsov, I.M., 2010. The conductivity structure across the Trans-European Suture Zone from magnetotelluric and magnetovariational data modeling, *Phys. Earth planet. Inter.*, **183**, 377–386.
- Kappler, K.N., 2012. A data variance technique for automated despiking of magnetotelluric data with a remote reference, *Geophys. Prospect.*, **60**, 179–191.
- Larsen, J.C., Mackie, R.L., Manzella, A., Fiordelisi, A. & Rieven, S., 1996. Robust smooth magnetotelluric transfer functions, *Geophys. J. Int.*, **124**, 801–819.
- Lezaeta, P., Chave, A. & Evans, R.L., 2005. Correction of shallow-water electromagnetic data for noise induced by instrument motion, *Geophysics*, **70**(5), G127–G133.
- Nowożyński, K., 2005. Tilt-Correction algorithm for Vector Magnetometers, *Publ. Inst. Geophys. Pol. Acad. Sc.*, **C-92**(379), 131–135.
- Pádua, M.B., Padilha, A.L. & Vitorello, I., 2002. Disturbances on magnetotelluric data due to DC electrified railway: a case study from southeastern Brazil, *Earth planets Space*, **54**, 591–596.

- Schmucker, U., 1970. *Anomalies of Geomagnetic Variations in the Southwestern United States*, University of California Press, Berkeley.
- Soyer, W. & Brasse, H., 2001. Investigation of anomalous magnetic field variations in the central Andes of N Chile and SW Bolivia, *Geophys. Res. Lett.*, **28**(15), 3023–3026.
- Worzewski, T., 2011. Marine magnetotellurics on a continental margin: imaging the hydration and dehydration cycle of the Costa Rican subduction zone, *PhD thesis*, Mathematisch-Naturwissenschaftliche Fakultät der Christian-Albrechts-Universität zu Kiel.
- Worzewski, T., Jegen, M., Kopp, H., Brasse, H. & Taylor, W., 2011. Magnetotelluric image of the fluid cycle in the Costa Rican subduction zone, *Nat. Geosci.*, **4**(2), 108–111.
- Worzewski, T., Jegen, M. & Swidinsky, A., 2012. Approximations for the 2-D coast effect on marine magnetotelluric data, *Geophys. J. Int.*, **189**, 357–368.

APPENDIX A

During the work on this data set, a number of hints on an inconsistency between the measurements of magnetic and tilt variations on the one hand and the total/ main magnetic field on the other hand has emerged. These hints are:

- (i) The difference between total field components after fluxgate magnetometer measurement and tilt-response function (Section 3.2.3 and Table 1),
- (ii) It has been tested if a substitution of the TRF elements by the correspondent measured total field values according to eqs (18)–(21) improves the noise removal in comparison to both the estimated TRF function and the modified one according to eq. (22), and the result was worst of all three cases,
- (iii) The unexpected result (Fig. 6) that the noise removal by the point-to-point re-rotation (an exact transform) is somewhat worse than by the tilt-response correction (an approximation),
- (iv) The dependency of tilt motion in the scalar total field F (Section 3.1, Fig. 2).

These points can be explained by lacking accuracy in the fluxgate-based total field measurement. For (i) and (ii), this is obvious, for (iii) and (iv) it has been confirmed by a simple test: Realistic, constant main field components H_0 and Z_0 have been subjected to an artificial periodic tilt motion $\alpha(t)$ in a realistic order of magnitude according to eq. (15). Both calculation of the scalar total field F and point-to-point re-rotation on these synthetic data resulted in constant time-series without traces of a dependency of α as expected. Then the time-series $H(\alpha(t))$ and $Z(\alpha(t))$ were shifted by constant values of 1 per cent of H_0 or Z_0 , respectively, to simulate an erroneous total field measurement. Now both calculation of F and re-rotation yielded varying time-series correlated to α with amplitudes close to the observed ones described in points 1 and 2.

A probable explanation for the problems with the total field measurement is that due to the compact construction of the offshore instruments, potential disturbing sources in the device itself are placed very close to the magnetometer sensor. Especially the battery is suspected of causing a DC shift in the magnetic records. Magnetized parts would have the same effect. However, we can exclude that induction effects due to some motion of the surrounding, electrically conducting sea water cause the problems described here, because we observed them also in magnetic time-series from fluxgates set in a similar periodic motion on dry land.

APPENDIX B

Here we present a rough outline how to derivate the tilt-response correction from the point-to-point re-rotation.

$\vec{B}(t)$ is the time-dependent magnetic field measured in the swinging coordinate system of the instrument, and $\vec{B}'(t)$ is the field in the fixed coordinate system that has a Z axis coinciding with the true vertical one. The point-to-point re-rotation transforms the first into the latter by means of a unitary operator \mathfrak{R}

$$\vec{B}'(t) = \mathfrak{R}(t)[\vec{B}(t)]. \quad (\text{B1})$$

The elements of the 3×3 matrix \mathfrak{R} are rather complicated expressions put together from sines and cosines of the tilt values α_x and α_y , see Nowożyński (2005) for details. The time-dependency of α_x and α_y causes that \mathfrak{R} is a time-dependent, too.

To introduce the approach we want to use in the tilt-response correction, we consider the inverse relationship first,

$$\vec{B}(t) = \mathfrak{R}^{-1}(t)[\vec{B}'(t)]. \quad (\text{B2})$$

Now, we divide $\vec{B}'(t)$ into a part containing the natural field variations relevant for magnetotellurics, and a mean, static part. Then the operator can be applied on the single terms of the sum separately. Utilizing that \mathfrak{R} and \mathfrak{R}^{-1} do not differ much from unity, we subsequently simplify the left-hand side of the sum by neglecting the effect of \mathfrak{R}^{-1} on $\vec{B}'_{\text{VAR}}(t)$,

$$\vec{B}(t) = \mathfrak{R}^{-1}(t)[\vec{B}'_{\text{VAR}}(t) + \vec{B}'_{\text{STATIC}}] \quad (\text{B3})$$

$$= \mathfrak{R}^{-1}(t)[\vec{B}'_{\text{VAR}}(t)] + \mathfrak{R}^{-1}(t)(\vec{B}'_{\text{STATIC}}) \quad (\text{B4})$$

$$\approx \vec{B}'_{\text{VAR}}(t) + \mathfrak{R}^{-1}(t)\{\vec{B}'_{\text{STATIC}}\}. \quad (\text{B5})$$

The last step means to disregard that the natural variations are subjected to the swinging of the coordinate system, and its validity is as better as smaller both the tilt and the natural variations are.

Taking into account that the static part of the magnetic field exceeds the variation part by 2–3 orders of magnitude and that the though small deviations of \mathfrak{R}^{-1} from unity are time-dependent, the right-hand side of the sum results in varying values of non-negligible size that are superimposed on the natural variations in the measured data. We call this part \vec{B}^{MOTION} in the following, whereas \vec{B}'_{VAR} is renamed with $\vec{B}^{\text{INDUCTION}}$ to emphasize its relevance for magnetotellurics and related induction methods,

$$\vec{B}(t) \approx \vec{B}^{\text{INDUCTION}}(t) + \vec{B}^{\text{MOTION}}(t). \quad (\text{B6})$$

A transition to frequency domain leads to eq. (7), and the subsequent explanation of $\vec{B}^{\text{INDUCTION}}$ with reference magnetic fields is (if we disregard complications due to a static coordinate transform) the well-known approach of the magnetovariational sounding method. The idea to explain \vec{B}^{MOTION} in an analogue way by means of $(\alpha_x, \alpha_y)^T$ has been motivated by a look at the very coherent tilt and magnetic data in Section 3.2.1. However, if comparing eqs (8) and (B5) now, this more intuitive approach turns out to be the linear approximation (i.e. a common first-order approach) of the operator \mathfrak{R}^{-1} . From this point of view it is not surprising either that the estimated tilt-response transfer functions TRF are closely connected to the components of the static field as demonstrated in Sections 3.2.2 and 3.2.3.